Journal of Engineering and Sustainable Development
Vol. 29, No. 02, March 2025
https://jeasd.uomustansiriyah.edu.iq/index.php/jeasd
ISSN 2520-0917
Research Article
https://doi.org/10.31272/jeasd.2646

Advancements in Ku Band Resonator Composite Right/Left-Handed (CRLH) Metamaterials: Design, Analysis, and Applications

Mustafa Mahdi Ali[1*], Enrique Márquez Segura[2], Taha. A. Elwi [3]

[1,2]Telecommunication Research Institute (TELMA), E.T.S. Ingeniería de Telecomunicación, Universidad de Málaga, Málaga, Spain
[3]Islamic University Centre for Scientific Research, The Islamic University, Najaf, Iraq

[*]Email: mustafa_mahdi@uma.es

Article Info

Received 02/05/2024
Revised 21/10/2024
Accepted 27/01/2025

Abstract

This paper comprehensively summarizes the Ku-band composite left-handed/right-handed (CRLH) resonator based on a 50 Ω two-ports network. A parametric simulation was provided based on CST MWS to reach the optimal design within the Ku-band. This design invokes two fractals based on Minkowski and Hilbert curves to realize the desired specifications. The proposed resonator performance was optimized according to the invoked fractal curves. After reaching the desired performance, the achieved results are validated. It is found that the resonator occupies an area of 35 × 30 mm^2 when printed on Roger RT5880 of 0.8 mm thickness with a complete ground plane. The resonator shows an excellent resonance near 15.45 GHz with an excellent quality factor. The evaluated S-parameters of the proposed resonator show minimum losses of about zero with a 30% reflection coefficient and 70% transmission coefficient. The numerical demonstration based on different numerical approaches, including HFSS, is mainly highlighted to quantify the efficiency of CRLH structures. In the end, it stated the present difficulties and the future work perspectives of the field, which explains the necessity of using complex applications and innovative design techniques to take advantage of all opportunists presented by CRLH in the Ku-band applications.

Keywords: Hilbert; Metamaterial; Minkowski; Resonator.

1. Introduction

Composite right-left-hand structure (CRLH) is one metamaterial (MTM) category. CRLH emerged as a promising area of research in microwave engineering, offering unique characteristics to design and manipulate electromagnetic waves at Ku band frequencies [1]. These structures are characterized by their simultaneous negative permittivity and permeability. CRLH exhibits unconventional electromagnetic properties that enable novel functionalities that are impossible with conventional materials [2]. Their ability to realize electromagnetic properties to the desired specifications leads to significant enhancements in various applications, including filters, antennas, absorbers, and phase shifters [3]. Consequently, depth development was recently improved for Ku band resonators-based CRLH antennas for satellite communications systems. This begins by testing the fundamental properties underlying CRLH inclusions and their mechanisms of operations in left-handed and right-handed behaviors [4]. Synthesizing RH and LH properties at certain frequency bands within a single unit cell offers manipulations with high flexibility and versatility for electromagnetic wave propagation for sensing applications, as reported in [5].

Ku band resonator design-based CRLH structures are a multi-layered development that adapts geometrical parameters, material characteristics, and structure configurations to accomplish the wanted electromagnetic properties [6]. Various design strategies based on a ranging transmission line approach to advance numerical optimization techniques were performed by efficient CRLH resonators with exceptional responses at Ku band frequencies [7]. Additionally, integrating materials with novel fabrication techniques enabled the realization of compact and lightweight CRLH structures to suit practical applications [8]. In addition to design specifications, analytical studies are very important for enhancing the functionality of Ku band resonators. Numerical simulations, such as finite element method (FEM) and finite difference time domain (FDTD) simulations, deliver the appropriate insights into CRLH behaviors and performance prediction [9].

A reconfigurable CRLH resonator based on a leaky-wave antenna was proposed for beam steering applications at Ku-bands to operate between 15 GHz and 16.2 GHz [10]. A miniaturized double negative CRLH to be oriented as an octagonal shape ring MTM to occupy an area of 9×9 mm^2 when printed on FR4 substrate to cover the frequency range from low bands up to 18 GHz [11]. Another design based on CRLH for bandpass filter applications using substrate-integrated waveguide technology was proposed in [12] to realize a bandwidth from 9.17 GHz to 20.31 GHz at 3 dB fractional bandwidth. Two defective ground structures based on CRLH inclusions were proposed for the ultra-wideband bandpass filter design operating at the Ku band using interdigital capacitors [13]. A Ku-band oscillator based on an air coaxial resonator at 11.6 GHz and output power of about -3.56 dBm [14]. A silicon-based coplanar waveguide line with four electric-LC resonators was introduced to form a wideband filter using CMOS technology to operate from 2 GHz to 18 GHz, with a band-stop frequency at 13.2 GHz and a rejection level of -40 dB [15]. A design of a compact wideband 6^{th} order elliptic Ku-band filter was implemented using Lithography-based Ceramic Manufacturing was proposed in [16]. A periodically polarized piezoelectric substrate was proposed to design a resonator using Aluminum Scandium Nitride materials to operate at Ku band systems that cover frequencies from 10.7 GHz to 18 GHz [17]. In [18], a fourth-order coaxial cavity resonator of a Chebyshev response was proposed to realize filter size reduction. Another filter design was fabricated using 3D printer technology that supports sophisticated, complex designs. A band stop filter was proposed from a complimentary ring resonator for Ku band applications to show a 3 dB Fractional bandwidth of 12.4% at a center frequency of 12.87 GHz [19]. A compact design manufactured for Ku bandpass filters with a central frequency of 14.25 GHz and bandwidth of 3.5%.

In light of these developments, a significant shortage was observed in investigating the use of CRLH/MTM for developing high-performance Ku band resonators. This is due to the effective losses of CRLH/MTM structures at high frequencies, including the Ku band between 12 GHz and 18 GHz. However, investigations of CRLH/MTM structures became urgent in the current state of the art due to their unique properties, which attracted different researchers worldwide.

Therefore, this work is realized to design CRLH/MTM for Ku band resonators. The proposed design is based on a fractal unit cell combination of Hilbert pair defective with Minkowski curves. The proposed unit cell is designed to match the applications at the Ku band by introducing the proposed unit cell to a 50 Ω transmission line with two ports. In section 2, the proposed resonator is developed and discussed with all geometrical details. The design methodology for all parametric studies to achieve optimal performance is developed in section 3. The achieved results are validated to realize the accuracy of the obtained results in section 4. The paper is concluded in section 5.

2. Resonator Geometrical Details

The proposed design is basically realized as a two-port network loaded with CRLH inclusions to realize microwave resonators at the Ku band. The proposed design is structured from an unmatched transmission line with two ports of 50 **Ω** sources. This is considered to ensure enough fringing from the transmission line toward the proposed CRLH structure [4]. The microstrip line is loaded to a CRLH structure with 5-unit cells. The individual unit cell is designed from a composite of a Hilbert pair separated by a Minkowski fractal curve based on the second order. Next, the design is printed on Rogers RT5880 with a thickness of 0.8 mm. The relative permittivity of the substrate is 2.2 with a loss tangent of 0.0009. The substrate is backed with a copper ground plane of 35 mm × 30 mm, as shown in Fig. 1. The transmission line width is 4 mm and is located 0.1 mm from the CRLH structure. Such a design is proposed to afford minimum losses due to radiation or conservation effects by optimizing the geometrical details to the dimensions in Fig. 1, as will be proven later. The effective resonance of the proposed structure with minimum losses is achieved at 15.45 GHz, as will be seen later. The Hilbert geometry is considered the second order, and the Minkowski is the second order fractal geometry.

Two software packages are invoked for this work to realize the optimal design. The first software package, CST MWS, optimizes the resonator design parametrically. Based on the HFSS formulation, the second software package realizes the validation outcomes obtained from CST MWS.

The main reason for that is to ensure loss reduction. The first fractal is based on capacitive effects, and the other is based on an inductive resonator. Both are designed to realize the same frequency resonance. Therefore, the impact of conservation losses can be eliminated significantly with this approach.

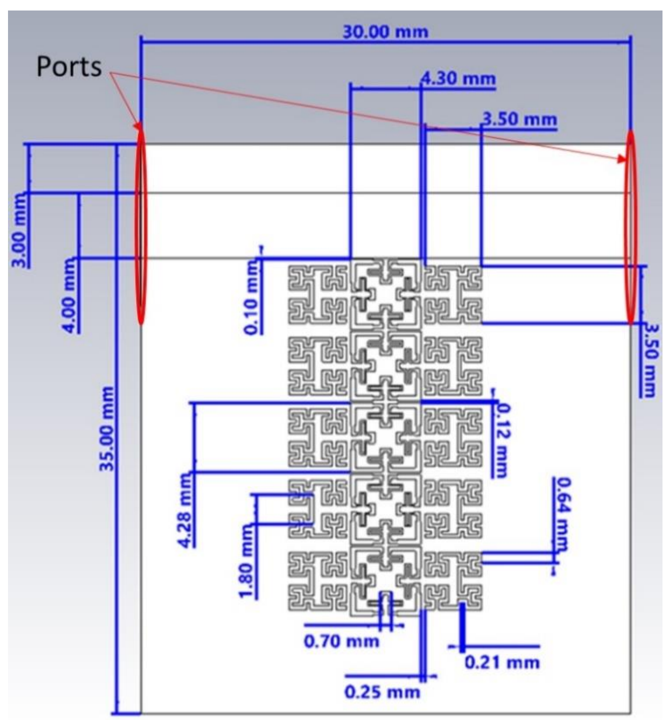

Figure 1. Resonator Geometrical details.

A complex and irregular iteration process can describe the proposed Minkowski fractal geometry dimensions through scaling an object size with a factor ε. Therefore, the Minkowski dimension (D)) can be approximated based on equation (1).

$$D = \lim_{\varepsilon \to 0} \left(\frac{log(N(\varepsilon))}{log(1/\varepsilon)} \right) \tag{1}$$

Where N is the minimum number of units needed to cover the fractal set. However, a parametric simulation often estimates the dimension (D) numerically. This involves covering the fractal parametric with a progressive variation in the side length and number scaling iterations at certain initials. However, reducing the limit as ε approaches zero increases the Minkowski dimension complexity, indicating a high filling space ratio.

The Hilbert curve can be defined as a space-filling geometry with a square area at a certain vertex that demonstrates self-similarity and non-integer recursively. The process continues until a desired level of detail can be reached. While there is no specific mathematical function, the recursive algorithm provides a systematic way to generate it. A parametric simulation can describe this to realize the desired performance. The side length of the individual segments for the Hilbert curve can be determined recursively based on the iteration level (i). For the Hilbert, the side length decreases by a factor of 2 with each iteration, starting with a base side length of 1. Therefore, the general equation for the side length L_i at the $i - th$ iteration can be expressed as in equation (2):

$$L_i = \frac{1}{2^i} \tag{2}$$

This equation captures the iterative refinement of the Hilbert curve, where each new iteration produces segments that are half the length of those in the previous iteration.

3. Design Methodology

In this section, the design methodology of the proposed resonator is discussed. As mentioned, the proposed resonator is structured in The transmission line structure and the proposed MTM load structure. The proposed MTM structure is consistent with two main inclusions: the Hilbert curve fractal of the second order and the Minkowski curve fractal of the second order. Each part of the proposed resonator has a specific influence that must be addressed during this section. Therefore, the proposed work was broken down by conducting a parametric simulation using the CST MWS environment. This parametric simulation is realized as follows:

3.1. Effective Distance influence (0.05 mm - 0.25 mm)

The effective distance describes the separation gap between the proposed transmission line and the MTM load. This distance is an effective parameter that realizes an electromagnetic coupling phenomenon between the conductive parts that are coupled to each other effectively in both capacitive and inductive effects. This is tested by varying this distance from 0.05 mm to 0.25 mm with a step of 0.05 mm using our proposed parametric simulation through monitoring the effects of that on the resonator S_{11} variations during the frequency band of interest. As seen in Fig. 2, the change in the obtained S_{11} results is recorded to realize the coupling effects between the proposed MTM and the transmission line. A significant decay was found in the resonance after increasing the distance over 0.1 mm. Such decay in the resonance frequency is due to the capacitive coupling reduction with increasing the separation distance [20]. Therefore, the distance was kept at 0.1 mm, which shows a minimum S_{11} within the frequency band of interest.

3.2. Horizontal Separation Distance (0.05 mm - 0.45 mm)

Now, the frequency resonance is monitored by evaluating the S_{11} parameter; this is adopted to realize the effects of the horizontal separation distance varying on the frequency resonance. Fig. 3 shows an observable change in the frequency resonance when introduced to such variation in this parameter. Such variation is due to the effects of the exponential phase retardation manner through the proposed MTM unit cells. Such phenomena were pointed out as the accumulation increase in the capacitive value over the entire MTM array between the Minkowski and the Hilbert structures. Again, at 0.25 mm, the proposed resonator shows the minimum S_{11} magnitude within the frequency band of interest.

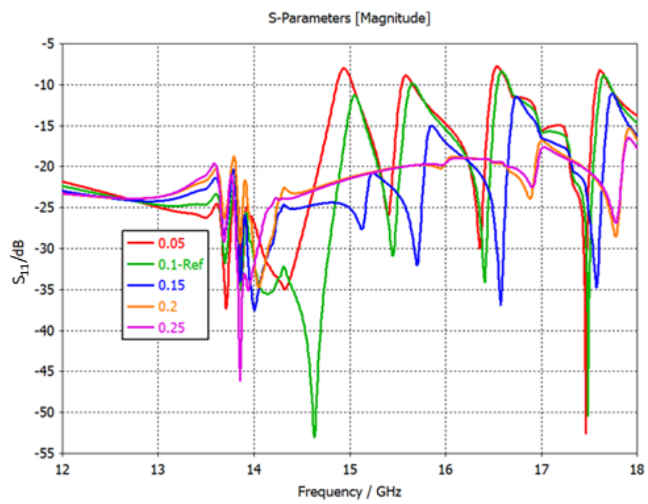

Figure 2. The evaluated S_{11} variation of the proposed resonator with changing the effective distance.

3.3. Vertical Separation Distance (0.02 mm - 0.42 mm).

Next, this part of the work discusses the variation in vertical separation distance. A minimum value of the S_{11} parameter was achieved at 0.12 mm. Such achievement is attributed to the effects of change in the unit cell periodicity, which directly affects the Brillion zone lattice and the frequency band gap. These observations are recorded on the evaluated S_{11} parameter in Fig. 4.

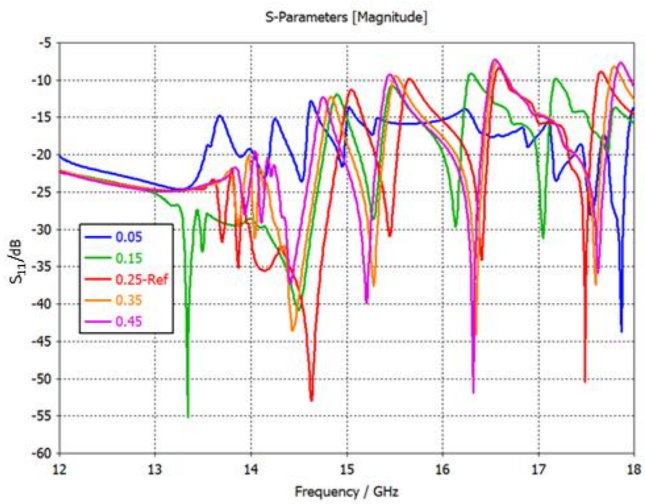

Figure 3. The evaluated S_{11} variation of the proposed resonator with changing the horizontal separation distance.

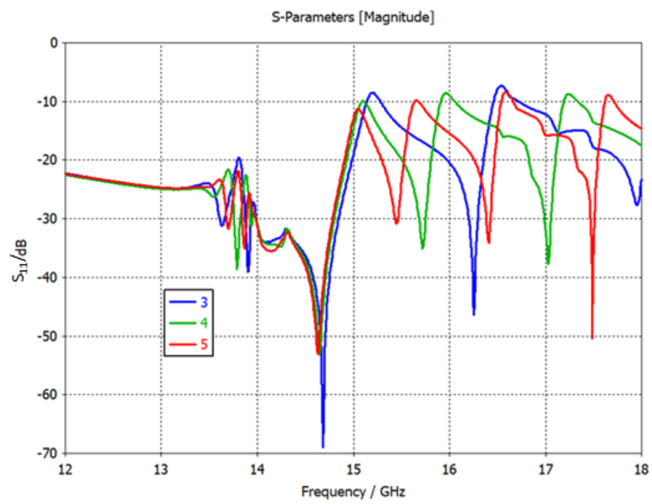

Figure 5. The evaluated S_{11} variation of the proposed resonator with changing the unit cell number.

3.4. Number of Unit Cells (3,4,5)

The effects of varying the unit cell number on the proposed resonator are discussed at a frequency resonance around 15.45 GHz. With increasing the unit cell, three observations are recorded: The first is defined by shifting the frequency resonance to the lower band till it reaches 15.45 GHz at the fifth unit cell introduction. The second observation is that upper and lower sidebands decay rapidly. The third is that the quality factor increases rapidly with unit cell numbers. These observations are attributed to increasing the capacitive-inductive branches in the effective resonance, significantly increasing the quality factor. Therefore, it is found from the recorded results in Fig. 5 that the proposed resonator performances are more desirable for us after reaching 5-unit cells. The observed phenomena could be increased by increasing the number of unit cells, but what has been achieved so far for our applications is satisfactory.

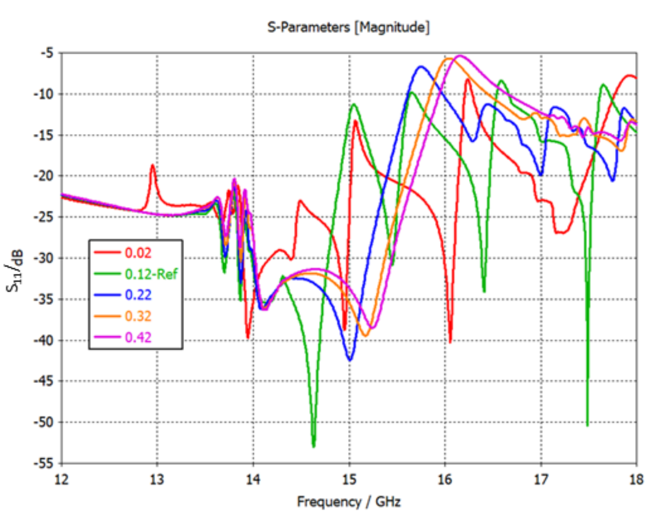

Figure 4. The evaluated S_{11} variation of the proposed resonator with changing the vertical separation distance.

4. Results and Discussions

After arriving at the optimal design from the previous section using CST MWS, the authors decided to validate their achievements using another software package based on HFSS. The evaluated results in Fig. 6 are shown in comparison to each other. The simulation results evaluated by the two considered software packages agree well. This agreement is achieved by setting the frequency range to Ku band frequencies, typically between 12 GHz and 18 GHz.

The mesh should be defined with enough accuracy according to the standard perfect matching layer boundary conditions to match minimum reflection at 10^{-9} factor with a distance from the structure edges of $\lambda/3$ at the desired frequency band through the open add space setup option. Using the mesh control tools to refine the mesh in critical areas such as near the feed point or any discontinuities, the energy criteria can be considered at -80 dB to ensure enough time for reaching the execution level. Specifying the excitation parameter for each port with direct coupling at each transmission line edge with enough embedding distance about three times the substrate height to ensure shielding effects. The solver settings of the appropriate options can be set to the Finite Integration Technique (FIT) and set up to the frequency sweep range and step size for the simulation within the band of 12 GHz to 18 GHz.

The second simulation software package uses the finest mesh to provide the accuracy sought in the first test to reach convergence of the resonator parameters in the frequency domain. Energy accuracy was limited to -80 dB, and a step of -10 dB was applied. It should be noted that only the required accuracy of 2% for simulations with HFSS can be achieved using an initial mesh of 18,987 tetrahedrals. A fast sweep option is applied with a linear frequency step starting from 12 GHz to 18 GHz with a step size of 0.1 GHz. In Fig. 6, the results obtained from both CST MWS and HFSS software packages agree well. It was found that the proposed resonator showed excellent resonance at 15.45 GHz with high selectivity.

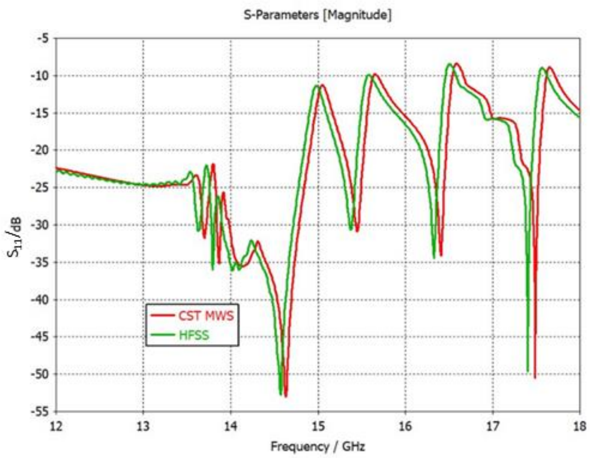

Figure 6. The evaluated S_{11} of the optimal design was validated using two different software packages.

Fig. 7 presents the proposed resonator's surface field distributions in terms of electrical field, magnetic field, and surface current. The proposed resonator shows an excellent field intensity on the proposed MTM structure that decays smoothly to the last unit cell.

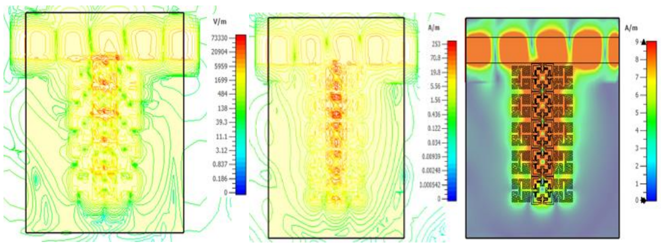

Figure 7. The evaluated field distributions.

Finally, the proposed design performance realized by the proposed design is compared to identical designs in the literature. Table 1 compares the proposed design performance in terms of area, bandwidth (BW), frequency (Freq), substrate, and loss rate. The comparison achieves an observable enhancement over the other related designs. It was found from this comparison that a significant loss reduction was achieved with the proposed design compared to the published designs.

Table 1. Comparison between the proposed resonator performance and the published results.

Ref.	Area (mm^2)	BW	Freq. (GHz)	Substrate	Loss
[21]	10× 10	K	21.6	FR-4	30%
[22]	10.4× 10.4	S, X, Ku	3.2, 5.32, 11.15, 16.73	FR-4	58%
[23]	8×8	X, Ku	8.5, 13.5, 17	Polyimide	53%
[24]	8.5× 8.5	Ku, K	15.52, 27.24	Polyimide	66%
[25]	8.5× 8.5	Ku	12.45, 14.18	FR-4	65%
The proposed work	30× 35	Ku	15.45	Roger	1%

5. Conclusions

In this work, a deep numerical simulation was applied based on parametric analysis and validation. The proposed work contains an informative analysis to realize the effects between the resonator parts. In this paper, the separation distances between the resonator parts were adjusted to determine the main effects of the proposed CRLH part on the proposed performance. By changing the unit cell number, a significant change in the proposed resonator performance is achieved in terms of frequency resonance and quality factor. The results show that the proposed resonator has no significant losses with acceptable S-parameters. The proposed resonator occupies an area of 35 × 30 mm^2 to achieve 15.45 GHz. The proposed resonator reflection coefficient is 30%, with a 70% transmission coefficient. Two numerical software packages, including CST MWS and HFSS, are invoked for this. The obtained results from the considered software packages agreed well. Finally, as a future work, this work will be exposed for experimental measurements for comparison.

Acknowledgments

This work is supported by the Telecommunication Research Institute (TELMA), E.T.S. Ingeniería de Telecomunicación, Universidad de Málaga. The authors also express their appreciation to the Journal of Engineering and Sustainable Development for the collaboration that made this work possible.

Conflict of interest

The authors declare that the publication of this article causes no conflict of interest.

Author Contribution Statement

Mustafa Mahdi Ali: Applied the theoretical simulations and performed the computations.

Enrique Márquez Segura: Proposed the research problem and supervised the findings of this work.

T. A. Oleiwi: Developed the theory and discussed the results.

References

[1]. M. Rahman, M. Islam, and M. Samsuzzaman, "Design and analysis of a resonator based metamaterial for sensor applications," *Microwave and Optical Technology Letters*, vol. 60, no. 3, pp. 694-698, 2018, doi: https://doi.org/10.1002/mop.31025.

[2]. R. K. Abdulsattar and T. A. Elwi, "A Theoretical Study To Design A Microwave Resonator For Sensing Applications," *Journal of Engineering and Sustainable Development (JEASD), 2nd online Scientific Conference for Graduate Engineering Students*, 2021, pp. 42-48, doi: https://doi.org/10.31272/jeasd.conf.2.1.6.

[3]. B. A. Esmail, S. Koziel, L. Golunski, H. B. A. Majid and R. K. Barik, "Overview of Metamaterials-Integrated Antennas for Beam Manipulation Applications: The Two Decades of Progress," *IEEE Access*, vol. 10, pp. 67096-67116, 2022, doi: https://doi.org/10.1109/ACCESS.2022.3185260.

[4]. V. Anitha, S. Palanisamy, O. I. Khalaf, S. Algburi, and H. Hamam, "Design and analysis of SRR based metamaterial loaded circular patch multiband antenna for satellite applications," *ICT Express*, Vol. 10, no. 4, pp. 836-844, 2024, doi: https://doi.org/10.1016/j.icte.2024.05.002.

[5]. A. I. Anwer, Z. A. A. Hassain, and T. A. Elwi, "A Fractal Minkowski Design for Microwave Sensing Applications," *Journal of Engineering and Sustainable Development*, vol. 26, no. 5, pp. 78-83, 2022, doi: https://doi.org/10.31272/jeasd.26.5.7

[6]. S. Ono et al., "Fabrication and measurement of 5 GHz miniaturized 10-pole bandpass filter using superconducting microstrip quasi-spiral resonators," *Physica C: Superconductivity*, vol. 468, no. 15-20, pp. 1969-1972, 2008, doi: https://doi.org/10.1016/j.physc.2008.05.112.

[7]. L. Gong et al., "A six-pole narrow-band high temperature superconducting filter with wide stop-band response at P-band," *Physica C: Superconductivity*, vol. 493, pp. 42-44, 2013, doi: https://doi.org/10.1016/j.physc.2013.03.017.

[8]. K. Yamanaka, M. Shigaki, and S.-i. Taira, "Ku-band HTS filters with narrow and wide bands for space communications," *Physica C: Superconductivity and its applications*, vol. 426, pp. 1638-1642, 2005, doi: https://doi.org/10.1016/j.physc.2005.04.030.

[9]. Z. Guoyong, F. Huang, and M. J. Lancaster, "Superconducting spiral filters with quasi-elliptic characteristic for radio astronomy," *IEEE Transactions on Microwave Theory and Techniques*, vol. 53, no. 3, pp. 947-951, 2005, doi: https://doi.org/10.1109/TMTT.2004.842485.

[10]. A. Sarkar, M. Adhikary, A. Sharma, A. Biswas, and M. J. Akhtar, "CRLH based leaky-wave antenna using modified Minkowski fractal on SIW with tunable frequency band," in *2017 IEEE Applied Electromagnetics Conference (AEMC)*, 19-22 Dec. 2017 2017, pp. 1-2, doi: https://doi.org/10.1109/AEMC.2017.8325650.

[11]. I. N. Idrus, M. R. Faruque, S. Abdullah, M. T. Islam, M. U. Khandaker, and J. Nebhen, "An octagonal split ring resonator-based double negative metamaterial for S-, X-and Ku-band applications," *Proceedings of the Institution of Mechanical Engineers, Part L: Journal of Materials: Design and Applications*, vol. 236, no. 11, pp. 2269-2280, 2022, doi: https://doi.org/10.1177/14644207211017155.

[12]. T. DURAISAMY, S. KAMAKSHY, S. S. KARTHIKEYAN, R. K. BARIK, and Q. S. CHENG, "Compact Wideband SIW Based Bandpass Filter for X, Ku and K Band Applications," *Radioengineering*, vol. 30, no. 2, 2021, doi: https://doi.org/10.13164/re.2021.0288.

[13]. J. Xie, D. Tang, Y. Shu and X. Luo, "Compact UWB BPF With Broad Stopband Based on Loaded-Stub and C-Shape SIDGS Resonators," in IEEE Microwave and Wireless Components Letters, vol. 32, no. 5, pp. 383-386, May 2022, doi: https://doi.org/10.1109/LMWC.2021.3136561.

[14]. Z. Zhan, Z. Xu, and C. Qian, "A Ku-band Oscillator Based on Air Coaxial Resonator," *2021 IEEE International Workshop on Electromagnetics: Applications and Student Innovation Competition (iWEM)*, Guangzhou, China, 2021, pp. 1-3, doi: https://doi.org/10.1109/iWEM53379.2021.9790596.

[15]. A. Rhbanou, S. Bri, and M. Sabbane, "Design of X-band substrate integrated waveguide bandpass filter with dual high rejection," *Microwave and Optical Technology Letters*, vol. 57, no. 7, pp. 1744-1752, 2015, doi: https://doi.org/10.1002/mop.29180.

[16]. P. Vallerotonda, L. Pelliccia, F. Cacciamani, C. Tomassoni and O. Bouzekri, "Additive-Manufactured TM01δ Mode Dielectric Resonators for Compact On-Board Wideband Filters," 2023 53rd European Microwave Conference (EuMC), Berlin, Germany, 2023, pp. 388-391, doi: https://doi.org/10.23919/EuMC58039.2023.10290540.

[17]. R. Vetury et al., "A Manufacturable AlScN Periodically Polarized Piezoelectric Film Bulk Acoustic Wave Resonator (AlScN P3F BAW) Operating in Overtone Mode at X and Ku Band," 2023 IEEE/MTT-S International Microwave Symposium - IMS 2023, San Diego, CA, USA, 2023, pp. 891-894, doi: https://doi.org/10.1109/IMS37964.2023.10188141.

[18]. M. Salek, X. Shang, and M. J. Lancaster, "Compact S -Band Coaxial Cavity Resonator Filter Fabricated By 3-D Printing," in *IEEE Microwave and Wireless Components Letters*, vol. 29, no. 6, pp. 382-384, June 2019, doi: https://doi.org/10.1109/LMWC.2019.2913155.

[19]. S. Ampavathina and V. Damera, "Compact Complementary Symmetric Ring Resonator Band Stop Filter for Ku band applications," *2022 IEEE Wireless Antenna and Microwave Symposium (WAMS)*, Rourkela, India, 2022, pp. 1-5, doi: https://doi.org/10.1109/WAMS54719.2022.9848080.

[20]. S.-F. Zhang *et al.*, "Design of dual-/tri-band BPF with controllable bandwidth based on a quintuple-mode resonator," *Progress in Electromagnetics Research Letters*, vol. 82, pp. 129-137, 2019, doi: https://doi.org/10.2528/PIERL18111305.

[21]. Z. B. Khan, Z. Huiling, G. Mehdi, and M. Y. Madni, "Design and measurement of cavity enclosed microstrip edge-coupled bandpass filter at ku band," in *2015 IEEE International Conference on Signal Processing, Communications and Computing (ICSPCC)*, 2015: IEEE, pp. 1-4, doi: https://doi.org/10.1109/ICSPCC.2015.7338919.

[22]. Y. Lei, S. Soo-Duk, C. Hak-Rae, and Y. Doo-Yeong, "Analysis of unit cells for filter design using CRLH transmission line," in *2012 Fourth International Conference on Communications and Electronics (ICCE)*, 1-3 Aug. 2012, pp. 397-401, doi: https://doi.org/10.1109/CCE.2012.6315937.

[23]. G. Shen and W. Che, "Compact Ku-band LTCC bandpass filter using folded dual-composite right-and left-handed resonators," *Electronics Letters*, vol. 56, no. 1, pp. 17-19, 2020, doi: https://doi.org/10.1049/el.2019.3033.

[24]. M. M. Ismail, T. A. Elwi, and A. Salim, "A miniaturized printed circuit CRLH antenna-based Hilbert metamaterial array," *Journal of Communications Software and Systems*, vol. 18, no. 3, pp. 236-243, 2022, doi: https://doi.org/10.24138/jcomss-2022-0030.

[25]. H. Hussein, F. Atasoy, and T. Elwi, "Origami Antenna Array Shaped Mosque Of Muhammed Al-Fatih For Visual Sight Enhancement In Modren 5g Mimo Networks," *Journal of Engineering and Sustainable Development*, vol. 27, no. 4, pp. 417-428, 2023, doi: https://doi.org/10.31272/jeasd.27.4.1.